Quantification of "Local" Surface Orientation: Theory and Experiment

Garth J. Simpson and Kathy L. Rowlen*

Department of Chemistry and Biochemistry, University of Colorado, Boulder, Colorado 80309

Received: August 18, 1998; In Final Form: December 3, 1998

To facilitate calculation of substrate roughness contributions to spectroscopically determined molecular orientation at surfaces, a scale-dependent method of determining the local surface normal tilt angle distribution is proposed and compared with experiment. Atomic force micrographs of fused silica were analyzed to determine the surface tilt angle distributions from the surface gradient. Good correlation between experiment and theory was observed for lateral separations comparable to the probe tip diameter. To overcome the tip-limited lateral resolution of atomic force microscopic roughness measurements, fractal analysis was used to extrapolate roughness values to molecular scales.

Introduction

Spectroscopic determination of molecular orientation at surfaces and interfaces can provide valuable insights into the nature and structure of surface systems. The orientation of surface molecules has been used to characterize two-dimensional phase transitions,[1] the structure of monolayer and multilayer films,[2] and the structure of interfaces.[3] Orientation is also a key parameter in construction of practical devices based on self-assembly technology, including thin films for use in nonlinear optics,[4,5] piezoelectric and pyroelectric detectors,[6] and chemical sensors.[6] In most practical applications, these mono- and multilayer films are constructed on surfaces which are not atomically flat. In such cases, surface roughness may influence the macroscopic orientation of the molecular films, and correspondingly alter interpretation of film structure and, thereby, the structure−function relationship.

While roughness contributions are often neglected in spectroscopic measurements of molecular orientation at solid surfaces, there is evidence that such contributions may not be negligible in many cases. For example, Burbage and Wirth considered the influence of surface roughness on the orientation of a probe molecule (acridine orange) at a fused silica/C18 surface in contact with water and water/alcohol solutions.[7] In that study, root-mean-square (R_q) roughness was measured by atomic force microscopy (AFM). When R_q values from analysis of a small scan size (20 nm × 20 nm) were used to estimate the contributions of roughness to the measured angular distribution, the contribution was found to be small (∼10%). However, when the R_q was determined from a larger scan size (400 nm × 400 nm), the contribution of surface roughness to the measured distribution in molecular orientation was found to be significant. In other studies, Firestone et al.[8] considered the influence of roughness on the spectroscopically determined orientation of surface-bound proteins on fused silica. AFM micrographs revealed a surface R_q of ∼15 Å for 1 μm × 1 μm scan sizes of the bare silica surface, comparable to values obtained in our laboratory.[9] Firestone et al. concluded that since R_q was less than the dimensions of the protein investigated (∼25 Å × 35 Å × 45 Å), surface roughness could be neglected.

Despite its use in the previous studies, R_q is not an ideal parameter to evaluate the influence of roughness on measured molecular tilt angles for several reasons. Most importantly, as shown in Figure 1, R_q values are highly dependent on length scale.[9−11] In fact, the exponential dependence of R_q on length scale is well documented and has been be used to determine fractal dimensions of surfaces.[10,11] As a result of this dependence, it is far from clear exactly which scan size, in AFM, yields a representative value of R_q for use in evaluating the role of roughness in the measured molecular tilt angles. Additionally, AFM roughness measurements of features much smaller than the tip diameter (∼5−40 nm) can be effectively smoothed by tip geometric effects.[12−14] Although multilayer surface films may be of thickness comparable to the tip diameter, most monolayer and submonolayer surface films are significantly less (∼1.5−3 nm), and therefore particularly susceptible to such tip-related artifacts. For these reasons, alternative methods of evaluating the contribution of surface roughness to molecular orientation are desired.

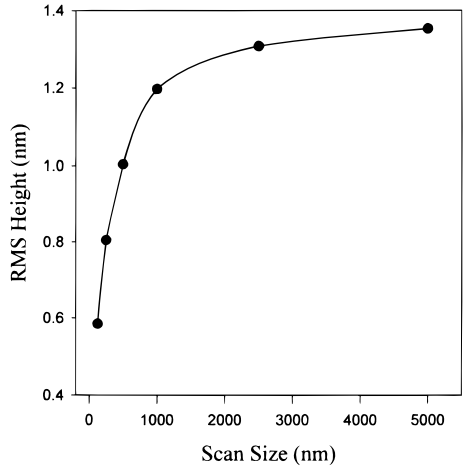

Figure 1. Root-mean-square roughness (R_q) of a fused silica slide as a function of square scan size in tapping mode AFM. All images were acquired at a scan rate of 2 Hz with minimal force (<1 nN). Typical relative error in R_q is 5−10%. The solid line is meant to serve as a guide to the eye.

The most useful roughness parameter for evaluating how surface structure contributes to spectroscopically determined molecular orientation is the distribution in surface slopes, i.e., the local surface normal tilt angle with respect to the macroscopic tilt angle. In this paper, a scale-dependent method of determining the local surface normal tilt angle probability distribution is proposed. The advantages of the theory/method result from its being (1) quantitatively accurate at both smooth

* To whom correspondence should be addressed.

10.1021/jp983396y CCC: $18.00
Published on Web 02/17/1999

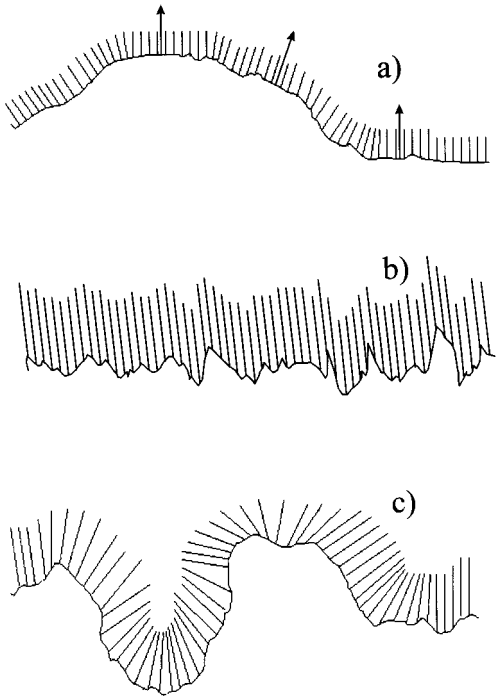

Figure 2. Illustration of surface feature influence on molecular orientation: (a) surface feature length scale much larger than molecular (vertical lines) length; the arrows represent the "local" surface normal, (b) surface features smaller than the molecular length, (c) surface features similar in size to molecular length.

and relatively rough interfaces, (2) reasonably simple to perform, and (3) based on easily obtainable roughness measurements.

Theory

Length Scale Considerations. As a first step in treating surface roughness contributions to spectroscopic molecular orientation measurements, it is useful to consider generally how substrate roughness affects molecular orientation. For tightly packed self-assembled monolayers in which orientation is determined by interactions between relatively long organic "tails" (e.g., octadecyl-), it is reasonable to assume that surface features much larger than the thickness of the monolayer are essentially flat with respect to the proximity of the molecule, as illustrated in Figure 2a. In this case, the tilt angle of the "local" surface plane would affect the molecular tilt angle with respect to a lab, or macroscopic, surface normal. Conversely, as illustrated in Figure 2b, surface features that are much smaller than the length of the molecule, or thickness of a monolayer, should not significantly affect molecular tilt within the monolayer. Of course, the transition region between these two extremes (i.e., for feature sizes on the order of the molecular length) is more difficult to treat, see Figure 2c. If this transition region is relatively narrow, such that features just larger than the molecular length are locally flat, and features just smaller are insignificant, then the contribution of surface features to the molecular tilt can be approximated by a step function at a particular cutoff length, Figure 3. The validity of this approximation is discussed in greater detail later in the text.

Molecular Tilt Angles. For molecules oriented on a locally flat surface feature, chemical interactions alone should dictate the degree of molecular tilt with respect to the local surface normal. If the local surface normal is aligned with the lab (or macroscopic) surface normal, the molecular tilt angle determined from spectroscopic measurements will provide an accurate probe of molecular orientation at the surface. If, however, the local surface normal is tilted with respect to the lab *Z* axis, as shown in Figure 4, macroscopic determination of the molecular tilt angle will yield a false result for molecular orientation on the surface.

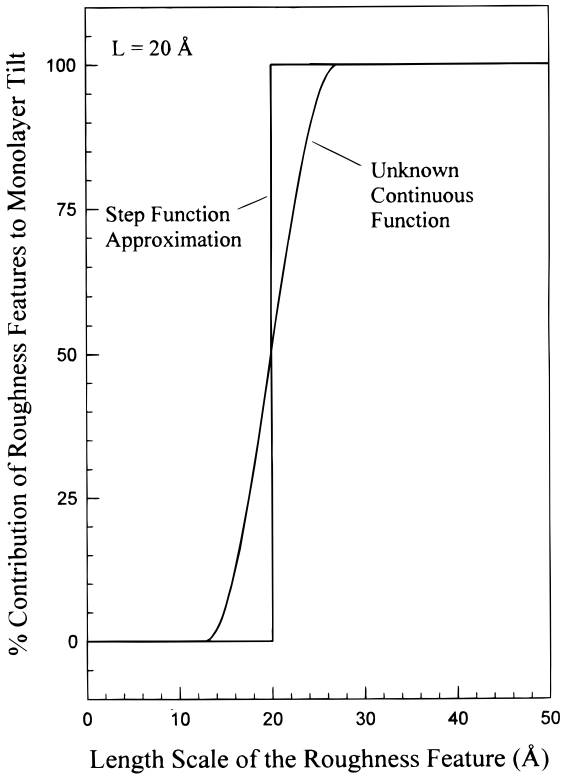

Figure 3. Graphical depiction of the step-function approximation for the roughness contribution to macroscopic molecular tilt. For features greater in size than the cutoff length (*L*), the surface is treated as locally flat, with a contribution to the observed macroscopic molecular tilt of 100%. Features smaller than the cutoff length are assumed to not contribute significantly to molecular tilt. Arguments are made within the text that, while the real function is unknown, it probably tracks reasonably well with the approximation.

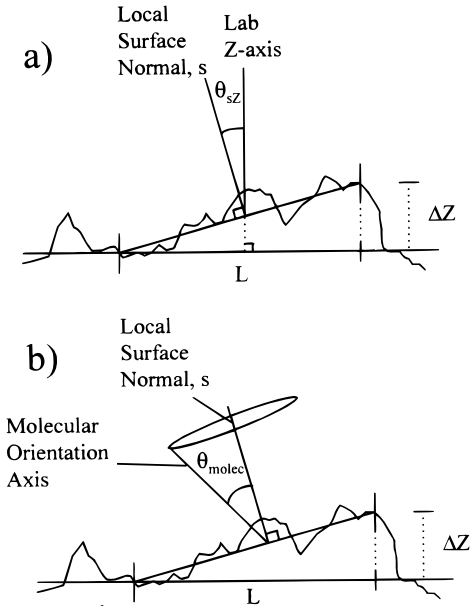

Figure 4. Illustration of relevant angles. The macroscopic normal is defined along the *Z*-axis of a macroscopic *X*,*Y* plane. The local surface normal (*s*) is defined from the slope between two vertical points separated by the cutoff length (*L*), i.e., $\Delta Z/L$. Assuming uniaxial molecular orientation, and the step function shown in Figure 3, it is possible to mathematically treat the distribution in surface "tilt" and the distribution in molecular "tilt" (θ_{molec}) separately.

Since, for locally flat surface features molecular orientation is determined solely by chemical interactions, it is possible to mathmatically treat the molecular tilt and the local surface tilt separately. The separability of the molecular distribution about the local surface normal and the distribution of local surface normals, is a direct consequence of the step-function approximation. The regions in which the approximation breaks down (i.e., if the surface feature size is comparable to the cutoff length) are also the regions where the two probability distributions are not expected to be independent of the value of the other. However, even if the model breaks down in this region, quantitative results may still be obtained provided that either the contribution drops sufficiently sharply in the neighborhood of the cutoff length or the influence of roughness is dominated by features much larger than the cutoff length. The accuracy of the step-function approximation is discussed in detail in later sections.

Direct Measurement of the Local Surface Normal Angle Distribution. Provided that the surface feature length is greater than, or comparable to, the probe diameter (i.e., AFM tip), such that tip geometric effects can be neglected, the local surface normal tilt angle distribution may be evaluated numerically directly from an AFM micrograph. The tilt angle distribution can be generated from the surface gradient evaluated at each accessible point at the surface.

$$F = f(X,Y) - Z = 0 \tag{1}$$

or

$$\nabla F(X,Y,Z) = (\partial f/\partial X, \partial f/\partial Y, -1) \tag{2}$$

where $f(X,Y)$ is the function describing the height Z at each (X,Y) location and $\nabla F(X,Y,Z)$ is the surface gradient at the point (X,Y). When analyzing a topographic image of finite resolution, calculations can be performed only at discrete separations. For example, when analyzing a 1 μm × 1 μm image with 512 points per line, the separation between each pixel is ~2 nm. Rewriting eq 2 in discrete format yields

$$\nabla F(X,Y,Z) \cong (\Delta Z/\Delta X, \Delta Z/\Delta Y, -1) \tag{3}$$

or

$$\nabla F(X,Y,Z) \cong \left[\frac{Z_{i,j+n} - Z_{i,j}}{L}, \frac{Z_{i+n,j} - Z_{i,j}}{L}, -1\right] \tag{4}$$

where $Z_{i,j}$ is the height of the pixel in the ith row and the jth column, n is the number of pixels between the analyzed points, and L is the lateral separation in nanometers between the points. L is equal to the separation between pixels multiplied by n. Once the gradient has been calculated, the local surface normal tilt angle θ_{sZ}, the angle between the gradient and the Z-axis, can be calculated by

$$\theta_{sZ} = \cos^{-1}\left(\frac{1}{|\nabla F|}\right) \cong \cos^{-1}\left[\left(\frac{Z_{i,j+n} - Z_{i,j}}{L}\right)^2 + \left(\frac{Z_{i+n,j} - Z_{i,j}}{L}\right)^2 + 1\right]^{-1/2} \tag{5}$$

The subscripts s and Z in θ_{sZ} indicate the local surface normal and the macroscopic surface normal, respectively. Use of eq 5, in conjunction with a height-based topographic AFM image, provides a direct measure of the 2D local surface normal tilt angle distribution.

Functional Form of the Local Surface Normal Probability Distribution. To compare the experimentally determined distribution in surface tilt angles with predicted values, it is necessary to develop a model for the probability distribution starting from measurable parameters, such as surface feature height. In many cases, rough surfaces are reasonably well described by Gaussian height distributions of the form[9,15]

$$P(Z,\sigma_Z) = (2\pi\sigma_Z^2)^{-1/2} \exp[-Z^2/2\sigma_Z^2] \tag{6}$$

$$\sigma_Z = \langle Z^2 \rangle^{1/2} \tag{7}$$

in which σ_Z is the root-mean-square roughness (R_q), Z is the height referenced to the mean surface height, P is the normalized probability of finding a particular height, and the brackets indicate an expectation value. The local surface normal tilt angle (θ_{sZ}) along one dimension in the surface plane is given by geometry to be the arctan($\Delta Z/L$). The probability of finding a particular slope along either the X- or Y-axes within the surface plane is equal to the probability of finding a particular difference in height over a known lateral separation. If only features of lateral size equal to or greater than the cutoff length (L) affect tilt, then the probability of finding a particular surface slope (in one dimension along the surface plane) is equal to the probability of finding a particular rise/fall ($(Z_1 - Z_2)$) over a lateral distance L, where Z_i is the height difference from the mean at a particular position (X_i, Y_i) in the $X-Y$ surface plane and Z_1 and Z_2 are separated by a distance L (see Figure 4). The variance, or squared root-mean-square, in the height difference g_z is then given by

$$g_z = \langle (Z_1 - Z_2)^2 \rangle = \langle Z_1^2 \rangle - 2\langle Z_1 Z_2 \rangle + \langle Z_2^2 \rangle = 2[\sigma_z^2 - \langle Z_1 Z_2 \rangle] \tag{8}$$

The expectation value for Z_1Z_2 is the autocovariance function of the surface (also called the height-height correlation function)[15] and describes the dependence of the height measured at Z_1 on the value of the height measured at Z_2. The distribution of height *differences* is also Gaussian and is given by

$$P(\Delta Z,\sigma_{Z,\text{eff}}) = (2\pi\sigma_{Z,\text{eff}}^2)^{-1/2} \exp[-\Delta Z^2/2\sigma_{Z,\text{eff}}^2] \tag{9}$$

$$\sigma_{Z,\text{eff}}^2 = g_z \tag{10}$$

in which ΔZ is the height difference and $\sigma_{Z,\text{eff}}$ is the effective width of the distribution after accounting for both the difference in height and the value of the autocovariance function (defined explicitly later in the text). Since tan θ_{sZ} equals $\Delta Z/L$, substitution of L tan θ_{sZ} for ΔZ into eq 9 yields the following expression for the one-dimensional distribution of local surface normal tilt angles

$$P_{1D}(\theta_{xZ},\sigma_{Z,\text{eff}}) = N_{1D} \sec^2 \theta_{sZ} \exp[-(L \tan \theta_{sZ})^2/2\sigma_{Z,\text{eff}}^2] \tag{11}$$

where N_{1D} is a normalization constant. The factor of $\sec^2 \theta_{sZ}$ results from changing the variable of integration to θ_{sZ} (the Jacobian of the coordinate transformation $d\Delta Z/d\theta_{sZ}$ is equal to $L \sec^2 \theta_{sZ}$, before normalization).

In Two-Dimensions. For AFM measurements made on an *area* of the surface rather than along a cross-section, the two-dimensionality of the surface plane must be included in roughness considerations. By analogy with calculation of a two-dimensional distribution of speeds, the two-dimensional tilt angle distribution is easily derived from the one-dimensional distribu-

tion by introduction of a geometric factor (before normalization) of $2\pi\theta_{sZ}$. This geometric factor (equal to the circumference of a circle of radius θ_{sZ}) effectively accounts for the "degeneracy" introduced by the second dimension; while only one combination yields a local surface tilt of zero (i.e., slopes along both *X*- and *Y*-axes simultaneously equals zero), nonzero tilt angles result from progressive combinations of tilts along the individual *X*- and *Y*-axes. The two-dimensional (2D) tilt distribution is given by

$$P_{2D}(\theta_{xZ},\sigma_{Z,\text{eff}}) = N_{2D}\,\theta_{sZ}\sec^2\theta_{sZ}\exp[-(L\tan\theta_{sZ})^2/2\sigma^2_{Z,\text{eff}}] \quad (12)$$

where N_{2D} is a normalization constant.

For cases in which the effective roughness $\sigma_{Z,\text{eff}}$ is small with respect to the cutoff length L, then the mathematics may be further simplified. For smooth surfaces and/or long cutoff lengths, the ratio of $\Delta Z/L$ will be small for most ΔZ, and

$$\theta^2_{sZ} = \arctan^2(\Delta Z/L) = \left[(\Delta Z/L) - \frac{(\Delta Z/L)^3}{3} + ...\right]^2 \cong (\Delta Z/L)^2 \quad (13)$$

Substitution of $L\theta_{sZ}$ for ΔZ in eq 9, and including the dimensionality of the system, yields the following approximate normalized distribution:

$$P_{2D}(\theta_{sZ},\sigma_\theta) \cong (1/\sigma^2_\theta)\theta_{sZ}\exp[-\theta^2_{sZ}/2\sigma^2_\theta] \quad (14)$$

$$\sigma_\theta = \sigma_{Z,\text{eff}}/L \quad (15)$$

where σ_θ is the root-mean-square tilt angle of the local surface normal in one dimension. The factor of $\sec^2\theta_{sZ}$ is not necessary in eq 14, as the Jacobian for the new coordinate transformation is simply the constant L. For relatively smooth surfaces, eq 14 predicts a Gaussian 2D distribution of local surface normal tilt angles modified by a preexponential factor of θ_{sZ}, with the parameter σ_θ easily calculated from the effective roughness. This approximate distribution is valid in the limit that $L \gg \sigma_{Z,\text{eff}}$.

Fractal Analysis for Feature Sizes Less Than the Tip Diameter. In instances in which the cutoff length is smaller than the tip diameter, including most molecular systems such as Langmuir−Blodgett films and self-assembled monolayers, the radius of curvature of the tip can introduce significant errors in the roughness measurements acquired by AFM.[12−14] It is therefore desirable to develop a method for extrapolation of measurements acquired at larger lateral separations to the regime below the instrument resolution. One such method is described here, in which AFM micrographs are treated by fractal analysis, allowing for the extrapolation of the surface tilt distribution to molecular scales.

In the previous discussion of the expected form of the two-dimensional local surface normal tilt angle distribution, the effective roughness ($\sigma_{Z,\text{eff}}$) was calculated from the variance in height difference (g_z) using eqs 8 and 10, in which the autocovariance function was introduced. In essence, the autocovariance function (or height-height correlation function) describes the correlation between heights on the surface as a function of the separation between them. If large-scale structure is present on the surface, then the probability of finding a particular height is not independent of the heights of the points adjacent to it. For example, if the surface is characterized by rolling "hills" and an initial point is at the top of a "hill", then the probability of finding a particular height at a separation much smaller than the hill size is highly correlated to the height at the top of the hill. However, at separations much larger than the average hill size, the two heights will no longer be significantly correlated.

Extrapolation of AFM roughness measurements to molecular scale may be achieved if an explicit functional form for the autocovariance function, $\langle Z_1,Z_2\rangle$, is used. A commonly used expression is the Kohlrausch−Williams−Watts function given by[16−17]

$$\langle Z_1,Z_2\rangle = \sigma^2_{z,\infty}\exp[-(L/\xi)^{2H}] \quad (16)$$

where H is a fractal scaling parameter, ξ is the lateral correlation length, and $\sigma_{z,\infty}$ is the asymptotic root-mean-square height evaluated at image sizes much greater than the correlation length. The exponent H is related to the local fractal dimension D by $D = 3 - H$.[17−19] For perfectly smooth, flat surfaces, $H = 1$ and $D = 2$, while for an entirely fractal surface (i.e., self-similar at all size scales), $H = 0$ and $D = 3$. Together with H, ξ determines the lateral distance required in order to "lose memory" of an initial height. Including the functional form for the autocovariance function into eq 8 yields the variance correlation function given as[17,18]

$$g_z(L) = 2\sigma^2_{Z,\infty}[1 - \exp[-(L/\xi)^{2H}]] = \sigma^2_{Z,\text{eff}} \quad (17)$$

The variance correlation function describes the probability of finding a particular variance (or squared root-mean-square) in height difference at a lateral separation of L. In the limit of $L \ll \xi$, eq 17 simplifies to the following expression:

$$g_z(L) \cong CL^{2H} \quad (18)$$

where

$$C \equiv 2\sigma^2_{Z,\infty}/\xi^{2H} \quad (19)$$

By determining the parameters $\sigma_{z,\infty}$, ξ, and H from experimental roughness measurements over a wide range of lateral separations, the variance correlation function may be extrapolated to molecular length scales. Once the scale-dependent variance in height difference has been determined, the local surface normal tilt angle probability distribution may be calculated by using eqs 8 and 10 in combination with either eq 12 or eq 14.

An additional advantage of fractal variance correlation function descriptions for surface roughness is that, in contrast to root-mean-square roughness, the roughness parameters are independent of scan size. This scan size independence was confirmed in our laboratory for measurements made by tapping mode AFM.[9] In fact, variance correlation functions can be calculated using combined data acquired for lateral separations ranging over 6 orders of magnitude in scale.[9]

Experimental Section

Tapping mode atomic force micrographs were obtained on a Digital Instruments nanoscope IIIa with etched single-crystal silicon tips (TESP, Digital Instruments). The tips/cantilevers had a nominal tip radius of 5−20 nm, ∼300 kHz resonance frequencies, and *Q*-factors of approximately 400. Tapping mode imaging conditions were as follows: scan rate 1.97 Hz, 512 points collected per line, *z* range equal to 2 nm, integral gain at 0.6 and proportional gain at 0.6. Images were acquired with the AFM located on an oil-suspended marble base (the base in Digital Instrument's top-view optical microscope) and all software-controllable filters were turned off. Prior to roughness

calculations the raw images were flattened (second order) using the modify/flatten subroutine in the nanoscope software (4.23r2). R_q was calculated using the analyze/roughness subroutine in the nanoscope software.

Fused silica (Esco, S1-UVB) was cleaned by sequential sonication (~5 min.) in 1.0 M potassium hydroxide, distilled water, hexanes, chloroform, and methanol. After cleaning, the fused silica surface was dried under a flow of USP nitrogen. Typical relative humidity in the laboratory was 30−50%. Force curves were acquired prior to, during, and after imaging in order to evaluate the nature and magnitude of tip-water layer-surface interaction. Observation of electrostatic attraction to the surface, coupled with very large pull-off forces, required the use of a polonium source (Static Master, 1c200) for discharge of the surface. The quality of each tip prior to analysis was evaluated by imaging either polystyrene nanospheres (50 nm diameter, tapping mode)[20] or a vapor deposited silver film (~5 nm thickness) on mica (contact mode).[21]

Prior to direct analysis of the local surface normal tilt angle distributions, AFM images were ASCII-exported as double-arrays of integers using the nanoscope software. The integer arrays were numerically converted from integer format to decimal format with units of nanometers, and the surface tilt angle calculated at each point using eq 5. The tilt angle histograms were generated by first evaluating the largest and smallest tilt angles, then setting a histogram bin size equal to 1/512 of the difference. Each measured tilt angle was compared with the bin angle as the bin angle was incremented from the minimum to the maximum. The first bin, for which the measured angle was greater than the bin angle, was then incremented by one, and the process repeated for each accessible pixel in the image.

In calculation of the variance correlation functions, ASCII-exported AFM images were again first numerically converted to decimal format with units of nm. To minimize noise due to scan drift along the slow scan axis,[18] variance correlation functions were determined by calculating the variance, $[Z_{ij} - Z_{(i+n)j}]^2$ along the lower-noise fast scan axis of the image double-array as a function of the separation in pixels, n (where Z_{ij} is the height at a particular ij pixel location). The calculation was repeated for every accessible pair of points in the 512 by 512 pixel image (at the edges some points are lost), and the average result was saved in an array as a function of the separation distance in nm. The process was then repeated for values of n up to 50 (for separations greater than one-fifth[18] to one tenth[22] the image size, variance correlation functions are no longer reliable), and the data arrays saved in separate files. The fractal exponential term H was determined by regressions of the linear portions of the log−log plots for scan sizes 250, 500, 1000 nm. The remaining two parameters, $\sigma_{z,\infty}$ and ξ, were determined by a least-squares fit of the 2500 and 5000 nm variance correlation functions to eq 17 using the fractal dimension determined from analysis of the smaller scan sizes.

Results and Discussion

Comparison of Theory and Experiment. As demonstrated in Figure 1, root-mean-square roughness measurements exhibit a strong scan size dependence, which can lead to ambiguities in quantitative evaluations of surface roughness based solely on R_q. An alternative to root-mean-square analysis, the fractal variance correlation function provides the scan size invariant parameters described in eq 17.

Figure 5 shows the variance correlation functions from tapping mode micrographs of fused silica. The data were obtained from scan sizes ranging from 125 nm to 5 μm. The inset plot shows the same data on a log−log scale. The solid line is a best fit of the combined data to the variance correlation function given by eq 17. In determining the best fit, the fractal exponential term H was determined by regressions of the linear portions of the log−log plots for scan sizes 250, 500, 1000 nm. The remaining two parameters, $\sigma_{z,\infty}$ and ξ, were determined by a least-squares fit of the 2500 and 5000 nm variance correlation functions to eq 17 using the fractal dimension determined from analysis of the smaller scan sizes. In this manner, values for H, ξ, and $\sigma_{z,\infty}$ were found to be (0.43 ± 0.02) (29.04 ± 0.02) nm, and (1.35 ± 0.02) nm, respectively.

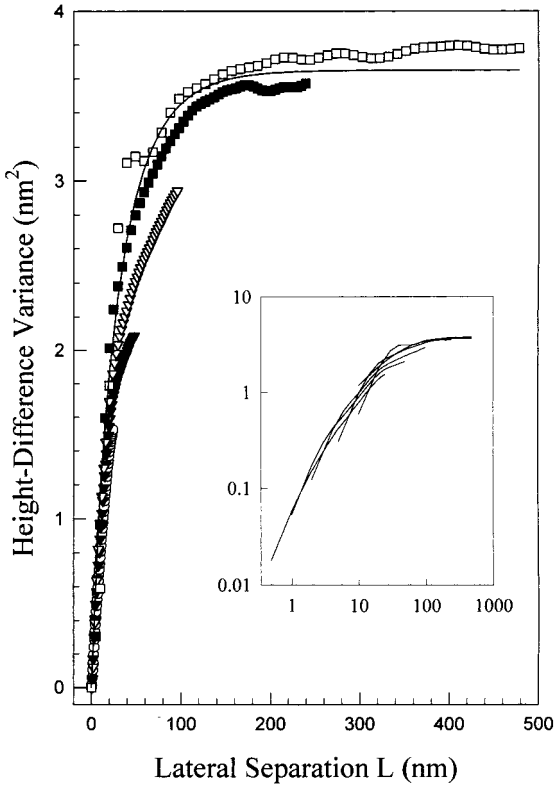

Figure 5. Fractal variance correlation functions for tapping mode micrographs of fused silica. The height-difference variance (defined in the text) is shown as a function of lateral separation is shown for a range of square scan sizes: solid circles = 125 nm, open circles = 250 nm, solid triangle = 500 nm, open triangle = 1 μm, solid square = 2.5 μm, open square = 5 μm. The solid line represents a best fit to eq 17, yielding the corresponding parameters $H = 0.43$, $\sigma_{z,\infty} = 1.35$ nm, and $\xi = 29.04$ nm. The inset plot displays the same data on a log−log scale (used in determining H).

If the surface were void of structure, and the height at each point independent of the heights of adjacent points, then a flat variance correlation function would be expected. Instead, the function is observed to be highly dependent on scale, at least for lateral separations of less than ~70 nm. This dependence on scale at the smaller separations suggests that the surface topography must be accounted for in reconstructing the tilt angle probability distribution, and that calculations based solely on the root-mean-square roughness would be inaccurate. The remarkable smoothness of the fused silica at scales greater than ~100 nm is intuitively appealing since the surface is optically flat and therefore not expected to have a significant number of roughness features comparable in size to the wavelength of light.

Palasantzas and Krim have demonstrated that variance correlation function analysis is quantitatively reliable for Gaussian height distributions.[17] In previous work, the AFM imaging conditions under which surface roughness is most accurately measured were determined.[9] While the data are not shown here, Gaussian height distributions on fused silica were observed when

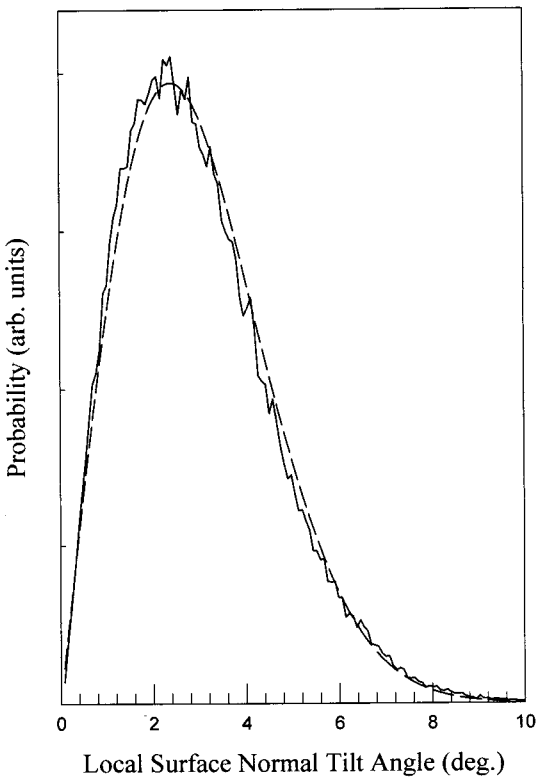

Figure 6. Comparison of theory and experiment. The solid line is the local surface normal tilt angle distribution experimentally measured from the gradient of a 1 μm × 1 μm AFM micrograph of fused silica. The dashed line is the same distribution calculated from scale dependent roughness using a cutoff length of 35 nm (or 18 pixels on a 1 μm scan). The squared correlation coefficient (r^2) is 0.998.

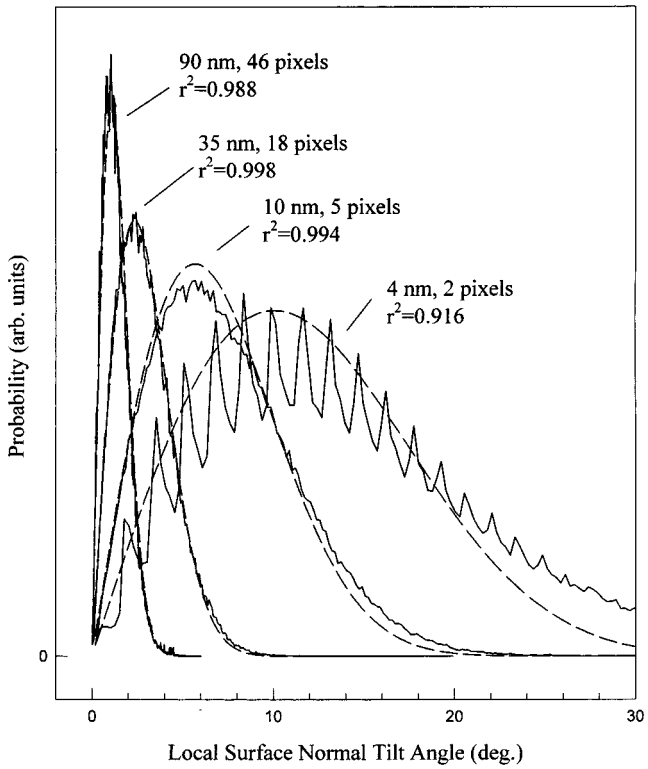

Figure 7. Comparison of measured (solid) local surface normal tilt angle distributions from a fused silica slide and the distributions calculated from the scale-dependent roughness (dashed lines) for a variety of lateral separations (90 nm, 35 nm, 10 nm, 4 nm). The quality of the fit decreases as the lateral separation decreases.

the scan speed limit for tapping mode AFM was not exceeded (such is the case for all data presented herein).

A representative comparison between the calculated and measured local surface normal tilt angle distribution for fused silica is shown in Figure 6. The measured distribution was acquired by gradient analysis of a 1 μm × 1 μm micrograph via use of eq 5. The calculated distribution was generated by the use of eq 12, with the effective roughness determined from fractal analysis (i.e., eq 17). In general, the theoretical form of the distribution function proposed in eq 12 correlates very well with the observed distribution at the larger cutoff lengths (with respect to the tip diameter).

Good correlation between the experimental and theoretical distributions is not always observed, however. In Figure 7 the measured distributions are compared with the calculated distributions for several lateral separations (L, in eq 5, also cutoff length in eq 12). For cutoff lengths of 35 and 90 nm, the measured tilt angle distribution functions are reproduced very well by the theoretical distributions. However, for the histogram acquired at a separation of 10 nm, deviations in the shape of the distribution are observed. At a separation of 2 nm, tip-induced geometric effects and other experimental artifacts combine to yield an experimental histogram which is almost certainly not representative of the surface. Clearly, for cutoff lengths on the order of a typical molecular size for monolayer films, the measured tilt angle distribution from the gradient is not reliable. In this case, the calculated distribution, derived from fractal analysis, is likely to provide a more accurate description of the surface normal tilt angle distribution. Of course, without accurate roughness measurements at molecular scales it is not possible to state this conclusion with great certainty. However, it is noteworthy that fractal descriptions of surfaces are typically valid over several orders of magnitude in scale.[23,24]

Evaluation of Approximations. An additional requirement for the model to yield quantitatively accurate tilt angle distributions is the reliability of the step-function approximation shown in Figure 3. Evidence supporting the validity of the approximation may be found in the success of other models using similar approximations. One well-known example is the Debye model for heat capacity of a crystal,[25] which has been very successful in predicting heat capacity in pure crystals and is based on assigning a cutoff length equal to the size of the atoms comprising the lattice sites for the wavelengths of phonon modes which may store heat. More relevant to roughness measurements, roughness at pure liquid surfaces modeled by capillary wave theory has been used to measure the cutoff length for wavelengths which may contribute to roughness to be 1.4 Å,[26] a length comparable to the size of a water molecule, 1.93 Å. In other studies, in which interfacial roughness at alkane/water,[27] alkane/monolayer/water,[28] and solid/monolayer/water interfaces[29] has been measured by fluorescence polarization anisotropy of an amphiphilic fluorophor, quantitative results were obtained by setting the cutoff length of roughness features equal to the size of the probe molecule. On the basis of the success of the cutoff length approximation in obtaining accurate results in other systems, it does not seem unreasonable to expect the same approximation to be successful in treating molecules at rough solid surfaces.

Further evidence supporting the accuracy of the cutoff length approximation may be found in Figure 8, in which the calculated tilt angle distributions are shown for several cutoff lengths. For changes in the cutoff length of 25%, the maximum in the distribution shifts at most not more than a few degrees. This fact demonstrates that the system is not particularly sensitive

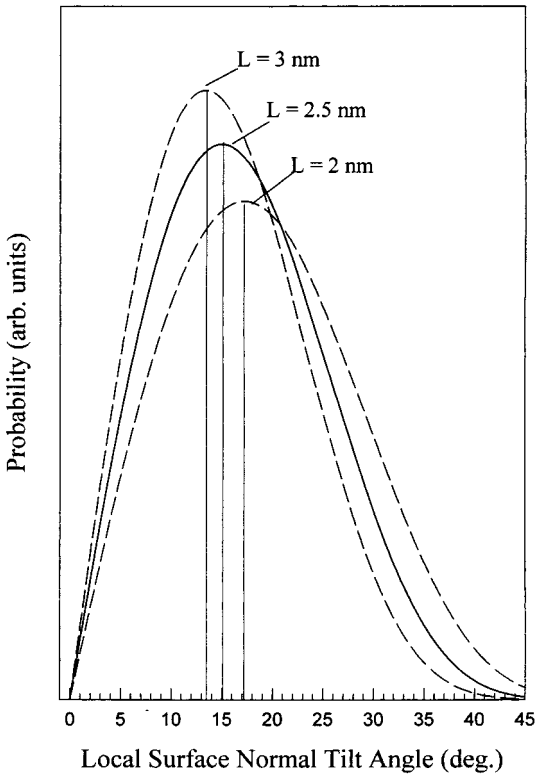

Figure 8. Three calculated local surface normal tilt angle distributions are shown for cutoff lengths of 3.0, 2.5, and 2.0 nm. These lengths were chosen as being representative of the typical size of molecules used for self-assembled monolayers. The calculated distributions were generated using the variance correlation function parameters fit from Figure 5 for a fused silica surface, $H = 0.43$, $\sigma_{z,\infty} = 1.35$ nm, $\xi = 29.04$ nm.

to roughness features in the neighborhood of the cutoff length, and that the bulk of the roughness contribution arises from features significantly larger than the cutoff length, even for an optically smooth surface such as fused silica. For surfaces which are much rougher (e.g., optically rough), an even greater proportion of the roughness influence will arise from features much larger than the cut-of length, with even less dependence on the cutoff length. Consequently, for surfaces at least as rough as optically flat polished fused silica, even if the step-function approximation is a poor one (which it is not expected to be), the quantitative result of the calculation will not be greatly affected by its failure.

Ramifications. Calculation of the local surface normal tilt angle distribution due to surface roughness provides a means to isolate and quantify the roughness contribution to a wide variety of orientation measurements. This can be accomplished by explicitly evaluating the experimental observables via integration over the separate distribution functions. Inspection of the surface normal tilt angle distribution calculated for a cutoff length of 20 Å (Figure 8), shows that the maximum in the distribution occurs at ~17°; a value well outside the experimental error of the techniques commonly used to measure molecular orientation at surfaces. Consequently, the contribution of surface roughness in spectroscopic investigations of molecular orientation is potentially significant, even for films prepared on optically flat substrates such as fused silica.

Summary. Taken together, the findings of this paper demonstrate that fractal variance correlation function analysis can provide a general means for accurately predicting the local surface normal tilt angle distribution, which, in turn, may affect orientation measurements of molecular and monolayer films. Variance correlation function fractal analysis is a widely applicable and well established method of quantifying surface roughness, and is valid over several orders of magnitude in separation distances, allowing for extrapolation to size scales below the instrument resolution. The two-dimensional local surface normal tilt angle distributions calculated from the fractal fit correspond well with the experimentally measured distribution at size scales greater than the tip diameter, and are expected to be representative of the surface at smaller size scales. The cutoff length approximation used to separate the roughness contributions from the local surface orientation for simple evaluation of spectroscopic measurements is reasonable for most rough surfaces. Consequently, the tilt angle distribution is relatively insensitive to changes in the cutoff length at size scales comparable to the thickness of a monolayer, and correspondingly insensitive to the cutoff approximation in general.

Acknowledgment. The authors gratefully acknowledge funding from the National Science Foundation.

References and Notes

(1) For example, see: (a) Enderle, Th.; Meixner, A. J.; Zschokke-Gränacher *J. Chem. Phys.* **1994**, *101*, 4365. (b) Lehmann, S.; Busse, G.; Kahlweit, M.; Stolle, R.; Simon, F.; Marowsky, G. *Langmuir* **1995**, *11*, 1174. (c) Zhang, D.; Gutow, J.; Eisenthal, K. B. *J. Phys. Chem.* **1994**, *98*, 13729. (d) Zhang, T.; Feng, Z.; Wong, G. K.; Ketterson, J. B. *Langmuir* **1996**, *12*, 2298. (e) Zhao, X.; Eisenthal, K. B. *J. Chem. Phys.* **1995**, *102*, 5818.

(2) (a) Shen, Y. R. *Annu. Rev. Phys. Chem.* **1989**, *40*, 327. (b) McGilp, J. F. *Appl. Surf. Sci.* **1993**, *63*, 99. (c) Bohn, P. W. *Annu. Rev. Meter. Sci.* **1997**, *27*, 469. (d) Bohn, P. W.; Walls, D. J. *Mikrochim. Acta* **1991**, *I*, 3.

(3) (a) Gragson, D. E.; Richmond, G. L. *Langmuir* **1997**, *13*, 4804. (b) Baldelli, S.; Schnitzer, C.; Shultz, M. J.; Campbell, D. J. *J. Phys. Chem. B* **1997**, *101*, 4607.

(4) Zyss, J. *Molecular Nonlinear Optics*; Academic Press: San Diego, 1994.

(5) Kajzar, F.; Swalen, J. D. *Organic Thin Films for Waveguiding Nonlinear Optics*; Overseas Publishers Association: Amsterdam, 1996.

(6) Ulman, A. *An Introduction to Ultrathin Organic Films: From Langmuir−Blodgett to Self-Assembly*; Academic Press: New York, 1991; pp 242, 251.

(7) Burbage, J. D.; Wirth, M. J. *J. Phys. Chem.* **1992**, *96*, 5943.

(8) Firestone, M. A.; Shank, M. L.; Sligar, S. G.; Bohn, P. W. *J. Am. Chem. Soc.* **1996**, *118*, 9033.

(9) Simpson, G. J.; Sedin, D. L.; Rowlen, K. L. *Langmuir* **1999**. In press.

(10) Williams, J. M.; Beebe, T. P. *J. Phys. Chem.* **1993**, *97*, 6249.

(11) Williams, J. M.; Beebe, T. P. *J. Phys. Chem.* **1993**, *97*, 6255.

(12) Westra, K. L.; Thomson, D. J. *J. Vac. Sci. Technol. B* **1995**, *13*, 344.

(13) Villarrubia, J. S. *Surf. Sci.* **1994**, *321*, 287.

(14) Reiss, G.; Vancea, J.; Wittmann, H.; Zweck, J.; Hoffmann, H. *J. Appl. Phys.* **1990**, *67*, 1156.

(15) Bennet, J. M.; Mattsson, L. *Introduction to Surface Roughness and Scattering*; Optical Society of America: Washington, DC, 1989.

(16) Williams, G.; Watts, D. C. *Trans. Faraday Soc.* **1970**, *66*, 80.

(17) Palasantzas, G.; Krim, J. *Phys. Rev. B* **1993**, *48*, 2873.

(18) Almqvist, N. *Surf. Sci.* **1996**, *355*, 221.

(19) Talibuddin, S.; Runt, J. P. *J. Appl. Phys.* **1994**, *76*, 5070.

(20) Ramirez-Aguilar, K. A.; Rowlen, K. L. *Langmuir* **1998**, *14*, 2562.

(21) Roark, S. E.; Rowlen, K. A. *Chem. Phys. Lett.* **1993**, *212*, 50.

(22) Oden, P. I.; Majumdar, A.; Bhushan, B.; Padmanabhan, A.; Graham, J. J. *J. Tribol.* **1992**, *114*, 666.

(23) Yehoda, J. E.; Messier, R. *Appl. Surf. Sci.* **1985**, *22/23*, 590.

(24) Rao, M. V. H.; Mathur, B. K.; Chopra, K. L. *Appl. Phys. Lett.* **1994**, *65*, 124.

(25) McQuarrie, D. A. *Statistical Mechanics*; Harper Collins: New York, 1976 (or any good statistical mechanics textbook).

(26) Pershan, P. S. *Faraday Discuss. Chem. Soc.* **1990**, *89*, 231.

(27) Wirth, M. J.; Burbage, J. D. *J. Phys. Chem.* **1992**, *96*, 9022.

(28) Piasecki, D. A.; Wirth, M. J. *J. Phys. Chem.* **1993**, *97*, 7700.

(29) Piasecki, D. A.; Wirth, M. J. *Langmuir* **1994**, *10*, 1913.

(30) The oscillations are believed to be an instrumental artifact and are a function only of the pixel separation.